Evaluating glacier fluctuations in Cordillera Blanca (Peru) by remote sensing between 1987 and 2016 in the context of ENSO

Walter SILVERIO[1] **and Jean-Michel JAQUET**[2*]

Ms. received the 7th March 2017, accepted 12th June 2017

Abstract

Six glacial cover maps of Cordillera Blanca in Peru were prepared using the band ratio (TM4/TM5) of Landsat 5 TM, ETM+4/ETM+5 of Landsat 7 ETM+ and OLI5/OLI 6_1 of Landsat 8 images. This cover varied between 618±60 km² in 1987 and 449±56 km² in 2016. In spite of differences in mapping methodologies, our glacial cover estimates are comparable with those of other studies, given an uncertainty margin of around ± 10 %. Since 1930, when the glaciers covered ca. 830 km², the Cordillera Blanca has lost 46 % of its cover in 86 years.

A nonlinear-, second-degree polynomial has been fitted to the glacier cover evolution overtime, showing that the negative rate of change has increased between the 80's (5 km² y⁻¹) and 2016 (23 km² y⁻¹). Considering altitude, the decrease in cover is particularly notable between 4500-5000 m and 5000-5500 m, and changes in the latter altitude are becoming more dominant over time (over 60 %). To explain the minor fluctuations in glacier cover around the global trend, the yearly rate of cover change was regressed against the mean Oceanic Niño Index for six periods between 1987 and 2016. The inverse relationship shows a certain amount of dispersion, that has yet to be explained, but is nonetheless significant.

Keywords: *remote sensing; Landsat; Snow index; band ratio; Andes; climate change; glaciology; El Niño/La Niña.*

Résumé

Evaluation des fluctuations de glaciers dans la Cordillera Blanca (Pérou) par télédection satellitaire entre 1987 et 2016 dans le contexte du phénomène El Niño/oscillation australe (ENSO). – *Six cartes de la couverture glaciaire de la Cordillera Blanca (Pérou) ont été élaborées sur la base des images numériques des satellites Landsat 5 TM (ratio TM4/TM5), Landsat 7 ETM+ (ratio ETM+4/ETM+5) et Landsat 8 (ratio OLI5/OLI 6_1). La superficie glaciaire a ainsi varié de 618±60 km² en 1987 à 449±56 km² en 2016. En dépit de quelques différences dans les méthodes cartographiques, nos estimations de couverture sont comparables avec celles d'autres auteurs étant donné une marge d'incertitude de ± 10 %. Depuis 1930, lorsque les glaciers recouvraient environ 930 km², la Cordillera Blanca a perdu 46 % de cette couverture en 86 ans. Un polynôme du deuxième degré ajusté à l'évolution de la superficie glaciaire montre que le taux de décroissance est passé de 5 km² y⁻¹ à 23 km² y⁻¹ entre les années 1980 et 2016. Considérant l'altitude, cette diminution de la couverture glaciaire est particulièrement importante entre 4500-5000 m et 5000-5500 m, et les changements dans cette dernière classe d'altitude sont désormais dominants (60 %). En vue d'expliquer les fluctuations mineures de la couverture autour de la tendance générale, le taux annuel de changement a été comparé avec l'Index Niño moyen (ONIm) pour six périodes entre 1987 et 2016 : les valeurs nettement négatives de l'index indiquent une prédominance de La Niña, provoquant une recrue*

[1] *UNEP DEWA/GRID Geneva, International Environment House, 11 Chemin des Anémones, 1219 Châtelaine, Switzerland*

[2*] *UNEP DEWA/GRID Geneva, International Environment House, 11 Chemin des Anémones, 1219 Châtelaine, Switzerland.* E-mail : jean-michel.jaquet@unige.ch

des glaciers (1997-2002 et 2011-2014), alors qu'une diminution de la surface glaciaire survient lorsque les épisodes El Niño dominent, marqués par une index positif (-23 km² y⁻¹ en 2015-2016). Bien qu'affectée d'une certaine dispersion qui reste à expliquer, la relation inverse trouvée montre bien l'influence de l'ENSO (El Niño / Southern Oscillation) qui module quelque peu la décroissance de la couverture glaciaire constatée depuis les années 1930 dans la Cordillera Blanca.
Mots-clés : *télédétection; Landsat; Indice de neige; ratios de canaux; Andes; changement climatique; glaciologie; El Niño/ La Niña.*

1. Introduction

In 1970, the Cordillera Blanca represented 35% of the ice cover of Peru. According to a second survey in 2003, the glacier surface represented about 40% of the national ice cover (UGRH 2013; 2010). Cordillera Blanca glaciers are one of the main reserves of freshwater for the region of Ancash. In 2005, one million people in this area were, directly or indirectly, dependent on its water resource for drinking water, agriculture, fish farming, electricity, and transporting mineral concentrates (Silverio 2007). Moreover, Cordillera Blanca waters irrigate the coast of the Ancash region through the CHINECAS project (an irrigation venture that includes the Chimbote, Nepeña, Casma and Sechin valleys). The waters are also captured beyond the Ancash region by the CHAVIMOCHIC irrigation project (including the of Chao, Virú, Moche, and Chicama valleys on the coast in the La Libertad region. This water is used to irrigate agricultural lands, generate electricity, and provide drinking water to the city of Trujillo (which had 500 000 inhabitants as of 2005) (Silverio 2007; Bury et al. 2013; Kaser et al. 2003). Thus, the disappearance of these glaciers would affect the lives of more than 1.5 million people and jeopardize agricultural exports for the whole region (Silverio 2007) (Fig. 1).

The cryosphere (snow, river and lake ice, sea ice, glaciers, ice caps, ice shelves, ice sheets, and frozen ground) reflects climate variations over a wide range of time scales, making it a natural record of climate variability that provides a visible expression of climate change. Recent decreases in ice mass have been correlated with rising surface air temperatures (Vaughan et al. 2013). Satellite imagery is an important source of information to map gla-

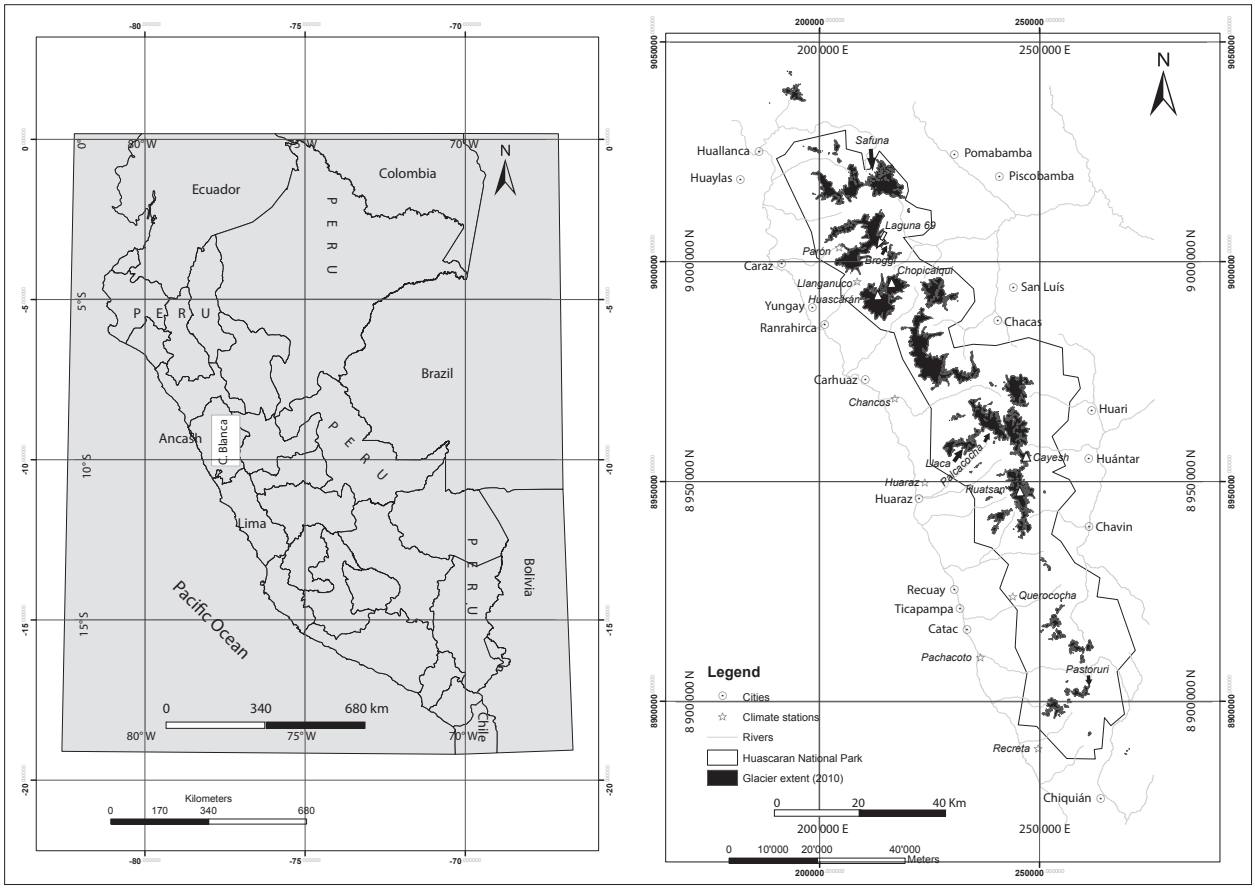

Fig. 1. Geographic position of Cordillera Blanca within Peru (left). Map of Cordillera Blanca with glacier cover in 2010 (right).

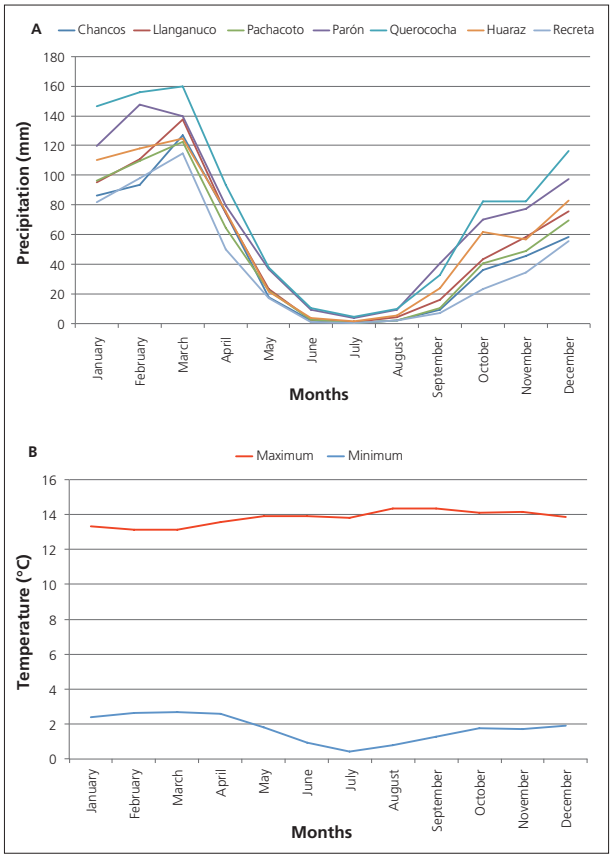

Fig. 2. Monthly precipitation and air temperature in Cordillera Blanca. (A) Multi-annual monthly mean precipitation in seven climate stations. (B) Multi-annual monthly mean temperature at Querococha climate station located at 4050 masl. Source of informations: Precipitation (B. Pouyaud, IRD, Montpellier, France, personal communication); temperature 1965-1986 (Ames, 1988), 1987-1993 (Abel Rodriguez, EGENOR, personal communication).

cier cover evolution due to its repeatability, synoptic character and easy integration into geographic information systems (Paul 2003). This is why remote sensing has been largely used to map glacier cover in Cordillera Blanca (e.g. Silverio and Jaquet 2005; Racoviteanu et al. 2008; Burns and Nolin 2014).

The present work has the following objectives: 1) to extend the time series of satellite-derived glacier cover maps to the year 2016, based on the imagery from Landsat 8-OLI instruments and document them by field observations; 2) to compare the cartographic results obtained by two spectral indices (NDSI and NIR/SWIR ratio) for 1987, 1996 and 2002 and evaluate the accuracy of glacial cover areal estimates; 3) to examine the distribution and evolution of glaciers with altitude; and 4) compare glacier fluctuations to the occurrence of El Niño Southern Oscillation (ENSO) events (El Niño / La Niña) until the last 2016 episode.

2. Location and general aspects of the Cordillera Blanca

The Cordillera Blanca is located between 08° 30' and 10° 10' S and between 77° 00' and 78° 00' W in the Peruvian Andean State of Ancash, 400 km north of Lima.

Topography, glaciers and climate are described more thoroughly in a previous study (Silverio and Jaquet 2005).

The climate of the Cordillera Blanca has been described by Kaser et al. (1990), Kaser et al. (1996) and Kaser and Osmaston (2002). It is characterized by two well-marked seasons: a wet season between October and April and dry season between May and September (Maussion et al. 2015; Schauwecker et al. 2014). The maximum precipitation occurs in March, and it remains below 20 mm per month during the austral winter (Fig. 2A). The monthly thermal amplitude at Querococha (4050 m) is almost constant throughout the year (Fig. 2B), but the daily variations are large: at 6000 m, in the absence of wind, the temperature may vary between -20°C in the early morning and +20°C at midday (Silverio 2003).

During the wet season, it rains every day in the valleys and snow falls at altitudes higher than 4800 m, but the tropical conditions (temperature and intense insolation) prevent any accumulation of snow outside the glaciers (Kaser et al. 2003). During the dry season, a few days with precipitation are possible, which are locally called *cambio de luna*. During these episodes, snow may fall at altitudes higher than 4500 m. During the 80s, the Andean summer was characterized by good weather, but in 2013 and 2014, some days were cloudy or had snow falls at altitude higher than 4200 m and rain, and it was cold around 4000 m. Precipitation and low temperature are characteristic of neutral and cold phases of ENSO (for periods of warm, neutral, and cold phases of ENSO, see NOAA 2016). During the 70s and 80s ENSO cycles were about seven years long, but the intensity and frequency increased during the last decades of 20th century (Cai et al. 2015; Capotondi et al. 2013; Wagnon 2001).

In the Cordillera Blanca, glacial accumulation occurs during the wet season, while ablation occurs throughout the entire year (Kaser et al. 1990; Francou and Wagnon, 1998). According to Ames et al. (1988), the Cordillera Blanca comprised 711 glaciers with a total surface of 721 km^2 in 1970 (excluding the small mountain ranges of Rosko and Pelagatos: see Silverio and Jaquet 2005). In 2003, there were 755 glaciers, because some of them experienced a fragmentation; their total surface was 528 km^2 (UGRH 2013; 2010).

Table 1. Characteristics of satellite imagery.

Satellite/Sensor	Date	Path/Row	Pixel (m)	Mapping/monitoring	Source
Landsat 2 / MSS MSS: Multispectral Scanner System	4 August 1975	8/66	60	Hazards, Glacier	UNEP/DEWA/GRID-Sioux Falls (USA)
Landsat 5 / TM TM: Thematic Mapper	31 May 1987	8/66, 8/67	30	Glacier cover	http://glovis.usgs.gov/
Landsat 5 / TM TM: Thematic Mapper	26 July 1996	8/66, 8/67	30	Glacier cover	http://glovis.usgs.gov/
Landsat 7 / ETM+: ETM+: Enhanced Thematic Mapper Plus	17 June 2002	8/66, 8/67	30	Glacier cover	http://glovis.usgs.gov/
Landsat 5 / TM TM: Thematic Mapper	18 August 2010	8/66, 8/67	30	Glacier cover	http://glovis.usgs.gov/
Landsat 8 / OLI OLI: Operational Land Imager	12 July 2014	8/66, 8/67	30	Glacier cover	http://glovis.usgs.gov/
Landsat 8 / OLI OLI: Operational Land Imager	30 May 2016	8/66, 8/67	30	Glacier cover	http://glovis.usgs.gov/

3. Data and methods

3.1. Image analysis

A total of seven images were used in this study, and their characteristics are given in Table 1. All images were mosaicked except for the 1975 MSS images, which covered only the northern part of Cordillera Blanca.

Geometric correction was performed on the 1987 image based on the Peruvian National Geographic Institute (IGN) 1:100 000 topographic map using 91 ground control points (GCPs) (Silverio and Jaquet 2005). This image was used for co-registration of the 1975 image. The rest of images used for glacier cover mapping were already in UTM and simply re-projected in zone 18 south.

The complex topography of the Cordillera produces strong shadow effects on the images and hence on the spectral signatures of land-cover classes (Silverio and Jaquet 2003; 2005). This effect could ideally be corrected through a topographic normalisation using a digital elevation model (DEM) (Dymond and Shepherd 1999), which should have a spatial resolution at least four times that of the image to be corrected (Sandmeier 1995). The DEM interpolated by Silverio (2007) using INRENA's contour lines (50-m resolution) does not meet this requirement. Previous studies attempting such a topographic normalization had poor results with over- and under-correction artefacts (Silverio and Jaquet 2003; 2005). We instead turned to band combinations or ratios for glacier cover mapping. Ratios and indices are known for their ability to eliminate, or at least to minimise, illumination differences due to topography (Colby 1991). They are calculated from visible and near-infrared channels with

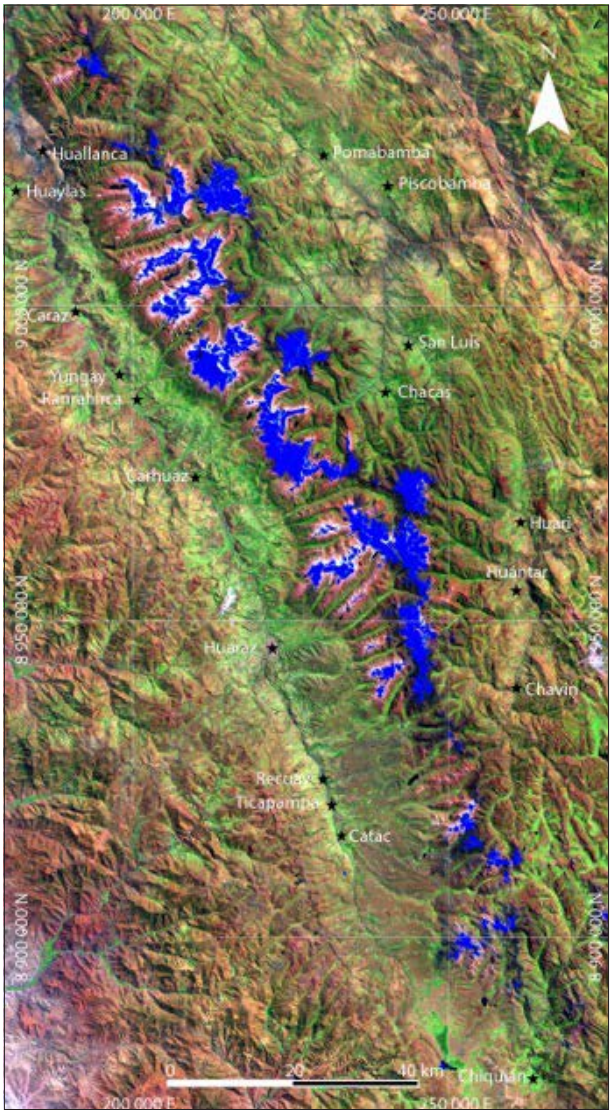

Fig. 3. Ratio image (2010) TM4/TM5 ≥ 2 showing Cordillera Blanca glaciers (blue). Background: composite image of Landsat5 TM of 18 August 2010 (RGB: 7/4/2).

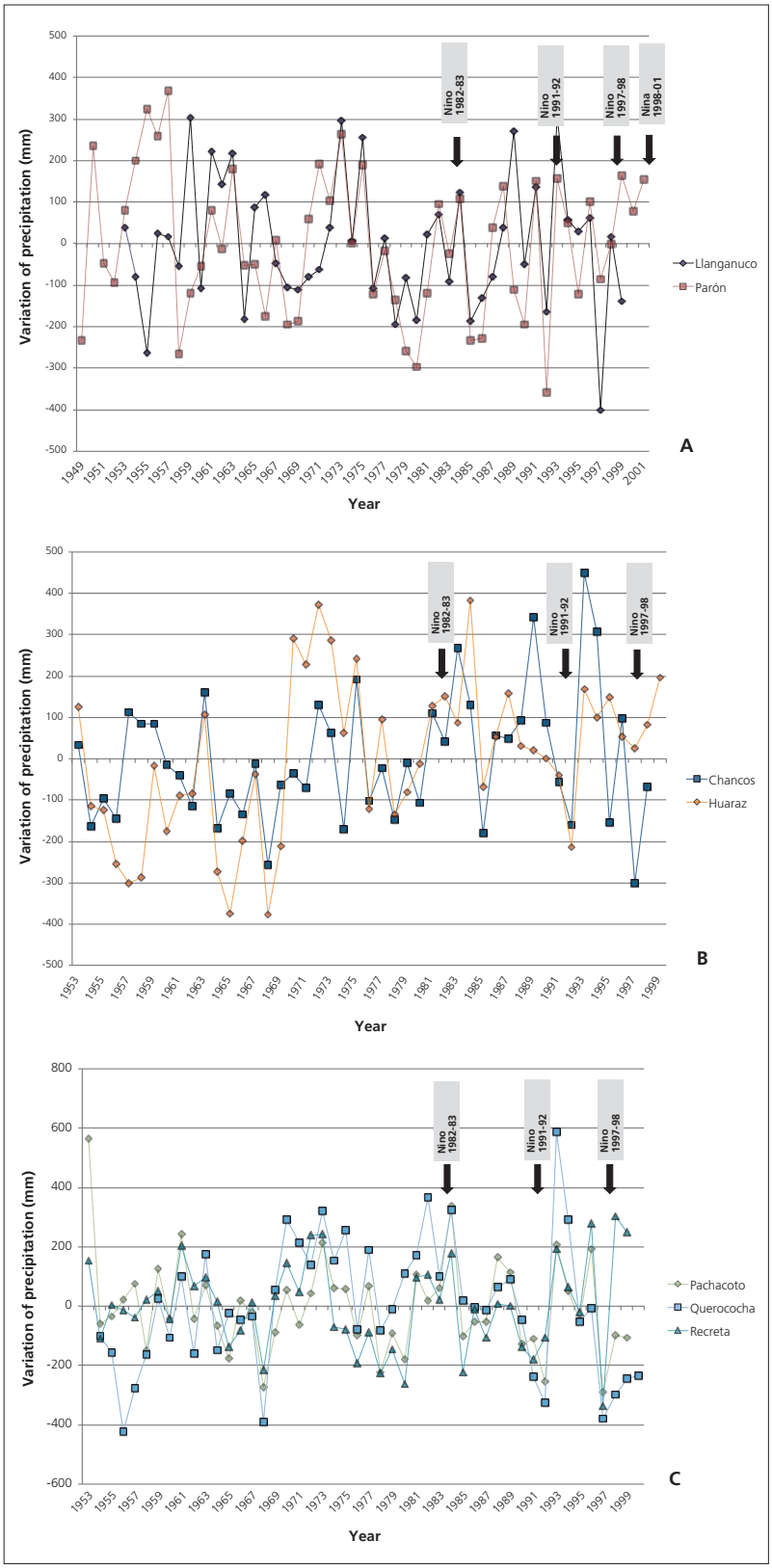

Fig. 4. Variation of precipitation during El Niño at climate stations of the Cordillera Blanca. A) North, B) Center and C) South.

low correlation, ideally, after eliminating additive noise (Bonn and Rochon 1993). However, since haze was not visible in the images, eliminating noise was deemed unnecessary (Silverio and Jaquet 2003; 2005). For mapping the years 1987, 1996, 2002, 2010, 2014, and 2016, we used the band ratios Landsat TM4/TM5, ETM+4/ETM+5, and OLI5 (0.845-0.885 µm)/OLI 6_1 [1,560-1,660 µm (IRM)]. The TM4/TM5 and ETM+4/ETM+5 ratios are spectrally equivalent according to NASA (2016), and they have commonly been applied in glaciology (Albert 2002; Paul 2002; Rees 2006). The Normalized Difference Snow Index (NDSI) (Hall et al. 1995; Silverio and Jaquet, 2003; 2005; 2009) was computed for the years 1987, 1996, and 2002 to enable comparisons with TM4/TM5.

The computations were carried out in Idrisi™ and yielded images in real mode, which were exported as integers into ArcView™ (ESRI). Glacier outlines were defined for TM4/TM5 ≥ 2, ETM+4/ETM+5 ≥ 2 and OLI5/OLI 6_1 ≥ 2. These values gave the best match with the glacier limits in the color composite image (TM RGB: 7/4/2; ETM+ RGB: 7/4/2; OLI RGB: 7/5/3; Fig. 3). The limits of the debris-covered glaciers were drawn on screen by visual inspection of the TM7/4/2, ETM+7/4/2 and OLI 7/5/3 composite images.

In contrast with our previous cartography (Silverio and Jaquet 2005), we have subtracted the rock outcrops present inside the glaciers from our cover estimates.

3.2. Other definitions

Individual ice bodies are defined in this work as portions of ratio images greater than or equal to a threshold of 2 with a surface area of 2700 m^2 (0.0027 km^2) or more (3 pixels).

The *uncertainty* of the area estimations was computed using the Perkal band method (Racoviteanu et al. 2008) which involves applying a one pixel-wide buffer on either side of the ice body limits.

In order to classify glaciers by *altitude*, we used the digital elevation model interpolated by Silverio (2007), which was resampled at a resolution of 30 m. The original contours spaced at 50 m were in geographic coordinates with altitudes ranging between 25 and 6700 m. After correction, the contours were reprojected onto UTM zone 18 South (Silverio 2007). The DEM was interpolated using TOPOGRID (Arc/INFO workstation). Within the Cordillera Blanca region, the altitude is between 1131 and 6701 m, but all glaciers are above 4000 m. We have defined five classes between 4000 and 6500 m and one beyond 6500 m. The glacier cover maps for 1987, 1996, 2002, 2010, 2014 and 2016 were rasterized at the same resolution and overlaid on the DEM to compute glacier cover by altitude.

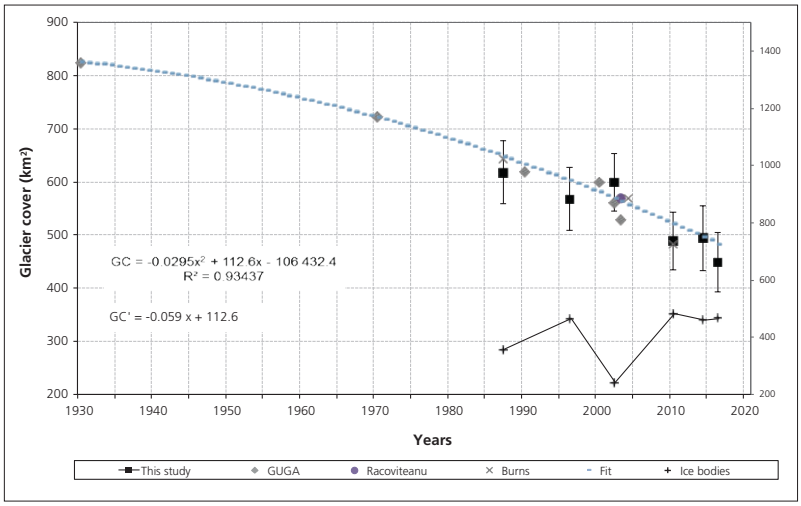

Fig. 5. Glacier cover evolution of Cordillera Blanca between 1930 and 2016. Crosses indicate the number of ice bodies, and the errors bars represent a ±1pixel uncertainty on the glacier limits. GC is the second degree fit on glacier cover, and GC' its first derivative, expressing an increase of negative rate of change of GC with time.

For a given altitude class and period, the *percent glacier cover change* (as shown in Table 4) represents the mean change (positive or negative) in glacier cover expressed as a percentage:

$$PGCC = 100 * \frac{GC_{\text{last}} - GC_{\text{first}}}{GC_{\text{i}}} \text{ [\%] } \{1\}$$

where GC_{first} is the glacier cover of the period's first year, and GC_{last} is the glacier cover for the last year.

3.3. Meteorological and climatic data

Fig. 2 shows representative precipitation and air temperature useful for understanding the glacier fluctuations in Cordillera Blanca. The data comprise multi-annual monthly patterns of precipitation for seven stations located in the Cordillera Blanca (Fig. 1 shows their locations) obtained from B. Pouyaud, IRD (Montpellier, France) and the monthly mean temperature at the Querococha climate station (located at 4050 m in the southern part of Cordillera Blanca; see Fig. 1). An illustration of the precipitation variability during El Niño/La Niña episodes is shown in Fig. 4.

In order to represent the ENSO phenomenon, the succession of El Niño/La Niña episodes is represented in Table 2 by the Oceanic Niño Index (*ONI*) computed by the NOAA (2016). *ONI* represents the three-month running mean (°C) of ERSST v4 (Extended Reconstructed Sea Surface Temperature) anomalies in the Niño 3.4 region (5°N-5°S, 120°-170°W).

3.4. Field observations

IRENA (now ANA: Autoridad Nacional del Agua/National Authority of Water) has surveyed the glacier front position for the Broggi glacier (1975-2002) and Pastoruri glacier (1987-2001). For the latter, additional front points were measured by GPS in 2008 and 2016, and field photographs were obtained (Figs. 6-9).

4. Results

4.1 Cordillera Blanca glacier cover between 1930 and 2016

Table 3 shows the available estimates that we have gathered for glacier cover in Cordillera Blanca. These were computed by various authors between 1930 and 2010 and by ourselves between 1987 and 2016 using TM4/TM5, ETM+4/ETM+5 and OLI5/OLI6$_1$ band ratios. Alternate estimations are also provided for 1987, 1996 and 2002 based on *NDSI*. The uncertainty (±) of the cover values is given in km^2 and % for band ratios images only. The number of ice bodies is in the last column.

Fig. 5 illustrates the multi-annual evolution of glacier cover and ice bodies. The decreasing trend is obvious, but there are small reversals in 2002 and 2014 with matching drops in the number of ice bodies. Over 46 years, the mountain range lost 272 km^2 of its ice cover. The rate of change

Table 2. Oceanic Niño Index (ONI) [3 month running mean of ERSST.v4 SST anomalies in the Niño 3.4 region (5°N-5°S, 120°-170°W)]. Black cell frame: beginning of the period; Mean, Stdev, Var coeff: for each period ONI mean, standard deviation and coefficient of variation.

	Dec Feb	Jan Mar	Feb Apr	Mar May	Apr Jun	May Jul	June Aug	July Sept	Aug Oct	Sept Nov	Oct Dec	Nov Jan	Mean	Stdev	Var coef %	N
1970	0.6	0.4	0.4	0.3	0.1	-0.3	**-0.6**	-0.8	-0.8	-0.8	-0.9	-1.2				
1971	-1.3	-1.3	-1.1	-0.9	-0.8	-0.7	-0.8	-0.7	-0.8	-0.8	-0.9	-0.8				
1972	-0.7	-0.4	0	0.3	0.6	0.8	1.1	1.3	1.5	1.8	2	1.9				
1973	1.7	1.2	0.6	0	-0.4	-0.8	-1	-1.2	-1.4	-1.7	-1.9	-1.9				
1974	-1.7	-1.5	-1.2	-1	-0.9	-0.8	-0.6	-0.4	-0.4	-0.6	-0.7	-0.6				
1975	-0.5	-0.5	-0.6	-0.6	-0.7	-0.8	-1	-1.1	-1.3	-1.4	-1.5	-1.6				
1976	-1.5	-1.1	-0.7	-0.4	-0.3	-0.1	0.1	0.3	0.5	0.7	0.8	0.8				
1977	0.7	0.6	0.4	0.3	0.3	0.4	0.4	0.4	0.5	0.6	0.8	0.8				
1978	0.7	0.4	0.1	-0.2	-0.3	-0.3	-0.4	-0.4	-0.4	-0.3	-0.1	0				
1979	0	0.1	0.2	0.3	0.3	0.1	0.1	0.2	0.3	0.5	0.5	0.6				
1980	0.6	0.5	0.3	0.4	0.5	0.5	0.3	0.2	0	0.1	0.1	0				
1981	-0.2	-0.4	-0.4	-0.3	-0.2	-0.3	-0.3	-0.3	-0.2	-0.1	-0.1	0				
1982	0	0.1	0.2	0.5	0.6	0.7	0.8	1	1.5	1.9	2.1	2.1				
1983	2.1	1.8	1.5	1.2	1	0.7	0.3	0	-0.3	-0.6	-0.8	-0.8				
1984	-0.5	-0.3	-0.3	-0.4	-0.4	-0.4	-0.3	-0.2	-0.3	-0.6	-0.9	-1.1				
1985	-0.9	-0.7	-0.7	-0.7	-0.7	-0.6	-0.4	-0.4	-0.4	-0.3	-0.2	-0.3				
1986	-0.4	-0.4	-0.3	-0.2	-0.1	0	0.2	0.4	0.7	0.9	1	1.1				
1987	1.1	1.2	1.1	1	0.9	1.1	**1.4**	1.6	1.6	1.4	1.2	1.1	**-0.06**	0.83	1455	204
1988	0.8	0.5	0.1	-0.3	-0.8	-1.2	-1.2	-1.1	-1.2	-1.4	-1.7	-1.8				
1989	-1.6	-1.4	-1.1	-0.9	-0.6	-0.4	-0.3	-0.3	-0.3	-0.3	-0.2	-0.1				
1990	0.1	0.2	0.2	0.2	0.2	0.3	0.3	0.3	0.4	0.3	0.4	0.4				
1991	0.4	0.3	0.2	0.2	0.4	0.6	0.7	0.7	0.7	0.8	1.2	1.4				
1992	1.6	1.5	1.4	1.2	1	0.8	0.5	0.2	0	-0.1	-0.1	0				
1993	0.2	0.3	0.5	0.7	0.8	0.6	0.3	0.2	0.2	0.2	0.1	0.1				
1994	0.1	0.1	0.2	0.3	0.4	0.4	0.4	0.4	0.4	0.6	0.9	1				
1995	0.9	0.7	0.5	0.3	0.2	0	-0.2	-0.5	-0.7	-0.9	-1	-0.9				
1996	-0.9	-0.7	-0.6	-0.4	-0.2	-0.2	-0.2	-0.3	**-0.3**	-0.4	-0.4	-0.5	**0.13**	0.76	566	110
1997	0	-0.4	-0.2	0.1	0.6	1	1.4	1.7	2	2.2	2.3	2.3				
1998	2.1	1.8	1.4	1	0.5	-0.1	-0.7	-1	-1.2	-1.2	-1.3	-1.4				
1999	-1.4	-1.2	-1	-0.9	-0.9	-1	-1	-1	-1.1	-1.2	-1.4	-1.6				
2000	-1.6	-1.4	-1.1	-0.9	-0.7	-0.7	-0.6	-0.5	-0.6	-0.7	-0.8	-0.8				
2001	-0.7	-0.5	-0.4	-0.3	-0.2	-0.1	-0.1	-0.1	-0.2	-0.3	-0.4	-0.3				
2002	-0.2	0	0.1	0.2	0.4	0.6	0.8	**0.8**	0.9	1.1	1.2	1.1	**-0.20**	-0.20	100	71
2003	0.9	0.7	0.4	0	-0.2	-0.1	0.1	0.2	0.2	0.3	0.3	0.3				
2004	0.3	0.3	0.2	0.1	0.2	0.3	0.5	0.6	0.7	0.7	0.6	0.7				
2005	0.7	0.6	0.5	0.5	0.3	0.2	0	-0.1	0	-0.2	-0.5	-0.7				
2006	-0.7	-0.6	-0.4	-0.2	0	0	0.1	0.3	0.5	0.7	0.9	0.9				
2007	0.7	0.4	0.1	-0.1	-0.2	-0.3	-0.4	-0.6	-0.9	-1.1	-1.3	-1.3				
2008	-1.4	-1.3	-1.1	-0.9	-0.7	-0.5	-0.4	-0.3	-0.3	-0.4	-0.6	-0.7				
2009	-0.7	-0.6	-0.4	-0.1	0.2	0.4	0.5	0.5	0.6	0.9	1.1	1.3				
2010	1.3	1.2	0.9	0.5	0	-0.4	-0.9	-1.2	-1.4	**-1.5**	-1.4	-1.4	**0.06**	0.67	1050	98
2011	-1.3	-1	-0.7	-0.5	-0.4	-0.3	-0.3	-0.6	-0.8	-0.9	-1	-0.9				
2012	-0.7	-0.5	-0.4	-0.4	-0.3	-0.1	0.1	0.3	0.3	0.3	0.1	-0.2				
2013	-0.4	-0.4	-0.3	-0.2	-0.2	-0.2	-0.3	-0.3	-0.2	-0.3	-0.3	-0.3				
2014	-0.5	-0.5	-0.4	-0.2	-0.1	0	-0.1	0	**0.1**	0.4	0.5	0.6	**-0.42**	0.43	103	47
2015	0.6	0.5	0.6	0.7	0.8	1	1.2	1.4	1.7	2	2.2	2.3				
2016	2.2	2	1.6	1.1	0.6	0.1	-0.3	-0.5					**1.10**	0.71	65	22

From NOAA (2016): http://www.cpc.noaa.gov/products/analysis_monitoring/ensostuff/ensoyears.shtml

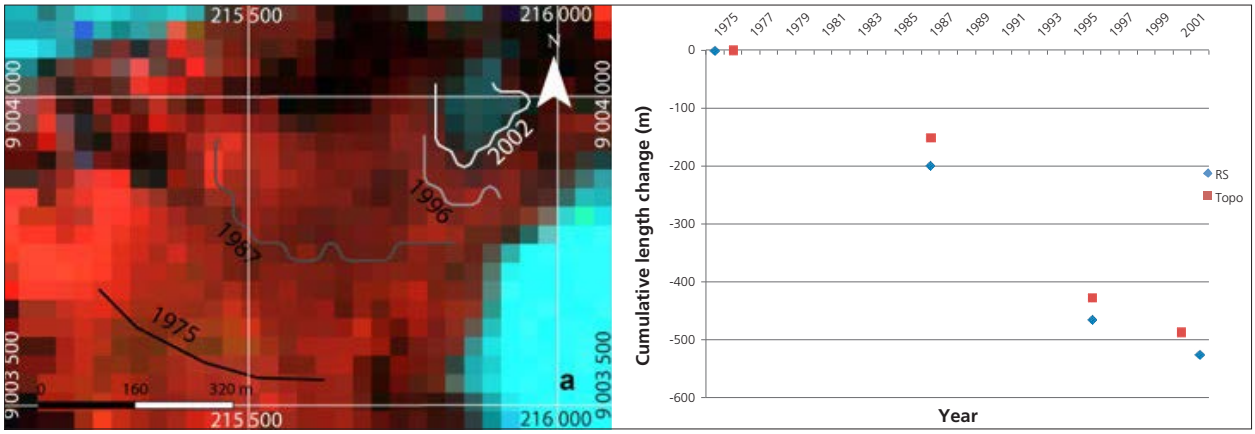

Fig. 6. (a) Evolution of the Broggi glacier front between 1975 and 2002. (b) Cumulative glacier retreat of Broggi by remote sensing (RS) between 1975 and 2002 and by topography (Topo) between 1976 and 2001. Field information comes from former INRENA (Peruvian National Institute of Natural Resources).

is given in Table 4C (*GCvar*) for the six periods defined since 1971. The rate becomes increasingly negative between 1971 and 1996 (around -5 km^2 year^{-1}), 2003 and 2010 (-14), and 2015 and 2016 (-23). This trend is reversed in 1997-2002 (5 km^2 year^{-1}) and in 2011-2014 (1.5 km^2 y^{-1}). A second-degree polynomial has been fitted to all the data points of Fig. 5 (*GC*) and its first derivative computed as *GC'* (in km^2 y^{-1}).

We illustrate the overall decrease in glacier cover with image and field data from two well-studied glaciers. The Broggi glacier retreated 500 m between 1975 and 2002 (Fig. 6) and completely disappeared in 2005, while the Pastoruri glacier shrank by 630 m between 1987 and 2014. It split into two ice bodies in 2007 (Figs. 7 and 8), and its retreat exceeded 100 m between 2008 and 2016 (Fig. 9). These two glaciers are examples of the general situation in Cordillera Blanca, where 81 % of glaciers had an area smaller than 1 km^2 in 2003 according to UGRH (2010).

4.2 Glacier cover distribution by altitude

For the period considered, less than 1 % of the Cordillera Blanca glacier cover exists between 4000-45000 m and above 6500 m (Table 4A). The majority (60 %) occurs between 5000-5500 m, about 20 % at 4500-5000 m and 15 % at 5500-6000 m (Fig. 10B). By altitude, the evolution has contrasting patterns over time (Fig. 10A) : omitting the extremes altitudes, there is a steady decrease of the cover at 4500-5000 m, a more irregular decrease at 5000-5500 m, and a small decrease at higher altitudes.

Table 3. Glacier cover in Cordillera Blanca between 1970 and 2016 as computed by various authors (left) and by this study (right; using NDSI *and* TM4/TM5*). In Km² and %. GUGA: George (2004), UGRH (2010a) and Ames et al. (1988); Rac: Racoviteanu et al. (2008); Burns: Burns and Nolin (2014). For Racoviteanu et al. (2008), figure in bracket is the uncertainty.*

	GUGA	Rac	Burns	This study NDSI Surface (Km²)	This study NDSI Uncert. (± Km²)	This study NDSI Uncert. (± %)	This study Ratio Surface (Km²)	This study Ratio Uncert. (± Km²)	This study Ratio Uncert. (± %)	Ice bodies
1930	825									
1970	721									
1987			644	632	Not estimated	Not estimated	618	60	10	357
1996				584	Not estimated	Not estimated	568	60	11	465
2000	600									
2002	560			591	Not estimated	Not estimated	599	54	9	241
2003	528	569 (21)								
2004			569							
2010			482				488	54	11	482
2014							494	61	12	459
2016							449	56	12	466

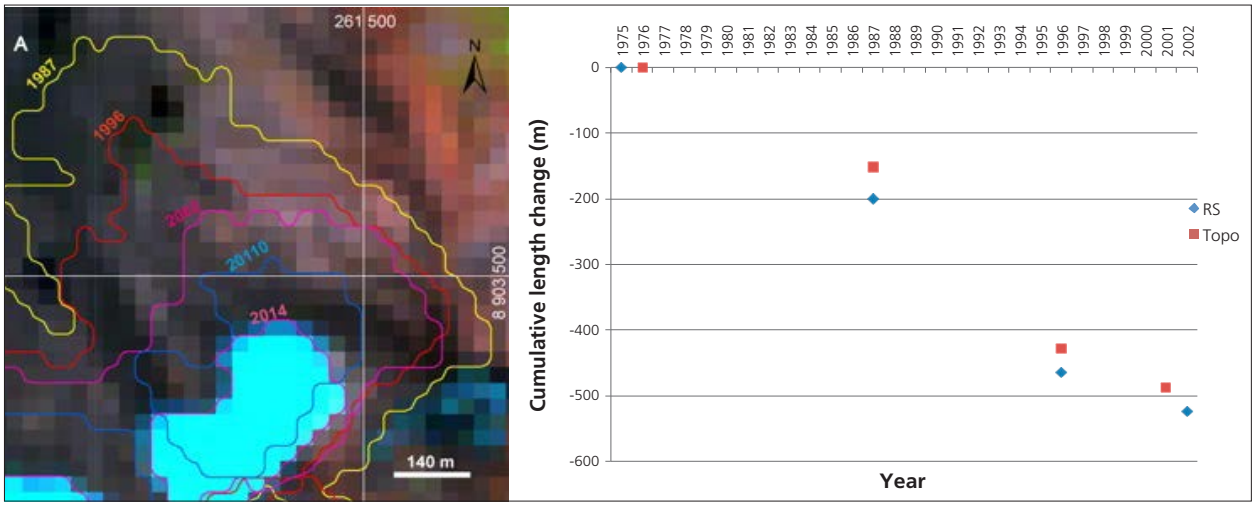

Fig. 7. (a) Monitoring of Pastoruri glacier from space between 1987 and 2014 with Landsat TM, ETM+ and OLI images. Color composites of 2014 OLI images (RGB: 6, 4, 2). (b) Cumulative glacier retreat of Pastoruri by remote sensing (RS) between 1987 and 2014 and by topography (Topo) between 1987 and 2001. In 2007, Pastoruri splits and later field measurements were discontinued. Field information comes from former INRENA (Peruvian National Institute of Natural Resource).

Table 4. Distribution of glacier cover GC *(A), percent glacier cover change* PGCC *(B) and glacier cover change per year* GCC *(C) by altitude between 1987 and 2016. PGCC is computed by formula {1} in text.*

A: GC											
Cumul. year			0	9	15	23	27	29			
Altitude (m.a.s.l.)	**1930 (km²)**	**1970 (km²)**	**1987 (km²)**	**1996 (km²)**	**2002 (km²)**	**2010 (km²)**	**2014 (km²)**	**2016 (km²)**	**2016-1987**	**2016-1970**	**2016-1930**
4000-4500			3.1	2.3	2.3	1.8	1.7	1.5	-1.6		
4500-5000			167.9	139.1	140.5	95.7	95.2	79.2	-88.7		
5000-5500			363.2	345.5	370.0	311.5	317.0	289.3	-74.0		
5500-6000			72.6	69.8	74.9	68.2	69.4	68.4	-4.2		
6000-6500			10.0	9.7	10.1	9.8	9.7	9.5	-0.5		
>6500			1.3	1.3	1.3	1.3	1.2	1.2	-0.1		
Total	**825**	**721**	**618**	**568**	**599**	**488**	**494**	**449**			
Change		-104	-103	-50	32	-111	6	-45	-169	-272	-376

B: PGCC								
Altitude (m.a.s.l.)	**1988-1996 (%)**	**1997-2002 (%)**	**2003-2010 (%)**	**2011-2014 (%)**	**2015-2016 (%)**	**2016-1987 (%)**	**2016-1970 (%)**	**2016-1930 (%)**
4000-4500	-26	2	-22	-8	-11	**-52**		
4500-5000	-17	1	-32	0	-17	**-53**		
5000-5500	-5	7	-16	2	-9	**-20**		
5500-6000	-4	7	-9	2	-1	**-6**		
6000-6500	-3	4	-3	-2	-1	**-5**		
>6500	-1	2	0	-5	-1	**-6**		
Total	**-8**	**6**	**-18**	**1**	**-9**	**-27**	**-38**	**-46**
% y-1	**-1**	**1**	**-2**	**0**	**-5**			

C: GCC							
Altitude (m.a.s.l.)	**1930-1970 (Km² y⁻¹)**	**1970-1987 (Km² y⁻¹)**	**1988-1996 (Km² y⁻¹)**	**1997-2002 (Km² y⁻¹)**	**2003-2010 (Km² y⁻¹)**	**2011-2014 (Km² y⁻¹)**	**2015-2016 (Km² y⁻¹)**
4000-4500			-0.1	0.0	-0.1	0.0	-0.1
4500-5000			-3.2	0.2	-5.6	-0.1	-8.0
5000-5500			-2.0	4.1	-7.3	1.4	-13.9
5500-6000			-0.3	0.9	-0.8	0.3	-0.5
6000-6500			0.0	0.1	0.0	0.0	-0.1
>6500			0.0	0.0	0.0	0.0	0.0
Gcvar	**-2.6**	**-6.1**	**-5.6**	**5.3**	**-13.9**	**1.5**	**-22.6**

Fig. 8. Evolution of Pastoruri between 2000 and 2016. Photos W. Silverio.

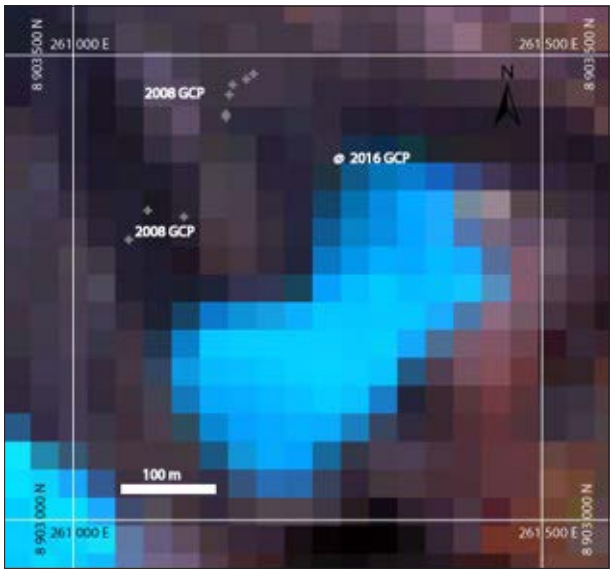

Fig. 9. Ground Control Points (GCP) taken in 2008 and 2016 with GPS show the Pastoruri glacier retreat was more than 100 m during this period. Colour composites of 2016 OLI images (RGB: 6, 4, 2).

The debris-covered glaciers (DCGs; see Fig. 11 for an example) are restricted to the four classes between 4000 m and 6000 m (Table 5; Fig. 12), with a strong predominance at 4500-5000 m. Between 1987 and 2016, the cover in this class decreases from 16 km² to about 13 km². A slight decrease occurs at 4000-4500 m, which matches a similarly weak increase at 5000-5500 m. The DCGs range from 60% to more than 90% of the *total* glacier cover at 4000-4500 m, with a smaller increase at 5500-5000 m and constant values at higher altitudes (Fig. 13).

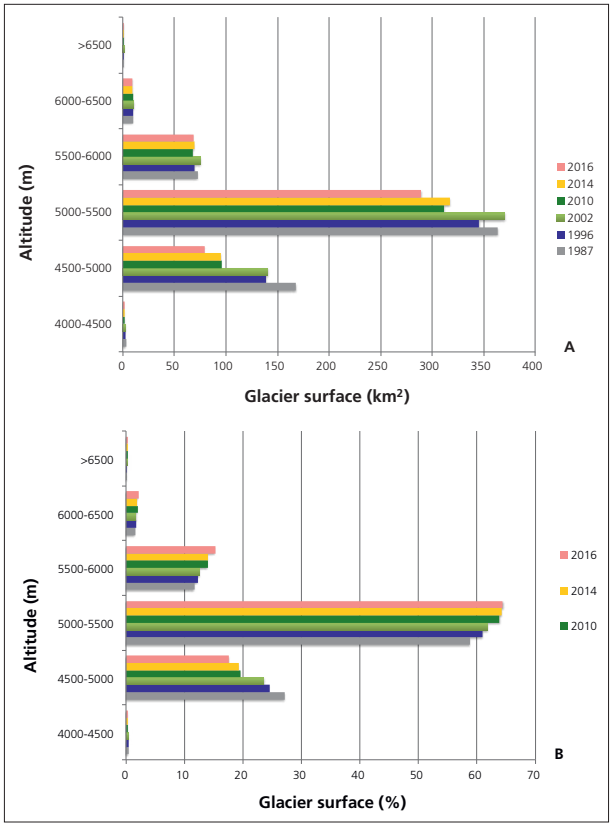

Fig. 10. Total glacier cover evolution by altitude between 1987 and 2016 (A) in km² and (B) in % computed over all altitude classes.

Table 5. Distribution of debris-covered glacier (DCG) by altitude between 1987 and 2016

Altitude (m.a.s.l.)	1987 (Km²)	1996 (Km²)	2002 (Km²)	2010 (Km²)	2014 (Km²)	2016 (Km²)	Diff (Km²)	change (%)
4000-4500	1.9	1.8	1.8	1.6	1.6	1.4	-0.5	-26
4500-5000	16.1	15.0	14.0	13.7	13.7	12.7	-3.3	-21
5000-5500	1.7	1.7	1.7	2.1	1.6	2.0	0.3	16
5500-6000	0.1	0.0	0.0	0.0	0.0	0.3	0.1	
6000-6500	0.0	0.0	0.0	0.0	0.0	0.0	0.0	
>6500	0.0	0.0	0.0	0.0	0.0	0.0	0.0	
Total	**19.8**	**18.4**	**17.5**	**17.4**	**16.8**	**16.4**	**-3.4**	**-17**

*Table 6. Glacier cover variation per year (*GCvar*) and mean value of* ONI *for six periods between 1971 and 2016*

Period	GC at period end (Km²)	Diff (Km²)	Duration (Y)	N months (m)	ONI (°C)	ONI CV (%)	GC var (Km² y⁻¹)
1970	721						
1971-1987	618	-103	17.0	204	-0.06	1455	-6.06
1988-1996	568	-50	9.2	110	0.13	566	-5.45
1997-2002	599	31	5.9	71	-0.20	100	5.24
2003-2010	488	-111	8.2	98	0.06	1050	-13.59
2011-2014	494	6	3.9	47	-0.42	103	1.57
2015-2016	449	-45	1.8	22	1.10	65	-23.48

4.3 Glacier cover change by altitude and period

The change in glacier cover by altitude (PGCC) computed for the five defined periods is shown in Table 4B and illustrated in Fig. 14. The variation follows two well-defined patterns. For the periods of 1988-1996, 2003-2010, and 2015-2016, PGCC is negative and monotonically decreases with altitude in a non-linear fashion. For 1997-2002 and 2011-2014, PGCC is globally positive and non-monotonic, with maximum change occurring between 4500 and 5500 m.

4.4. Glacier cover variation and ONI

Table 2 (rightmost columns) shows the average value of ONI (*ONIm*) computed for the six periods between 1971 and 2016, along with the standard deviation, coefficient of variation (*CV* in %), and sample size (number of months). The large *CV* indicates a high variability of *ONI* within each period. Table 6 lists these parameters and corresponding values of the glacier cover variation per year. The relationship between *ONIm* and *GCvar* is plotted in Fig. 15. The coefficient of determination (R^2 = 0.8) is significant at the 95% level.

6. Discussion

6.1. Influence of cartographic methodology and uncertainty on glacier evolution estimates

We have applied the *TM4/TM5 ratio* based on DNs to map the glacier limits between 1986 and 2010, as well as OLI5/OLI6 for 2014 and 2016, which have equivalent spectral bands. The *TM4/TM5* ratio is commonly used in glaciological studies (Hall et al. 1987; Paul 2002; Paul et al. 2002; Paul et al. 2004; Williams et al. 1991), and it is simpler to compute than *NDSI*. According to Paul (2000), this ratio gives the best results for glacier mapping, especially in shadowed areas. Albert (2002) shows a difference

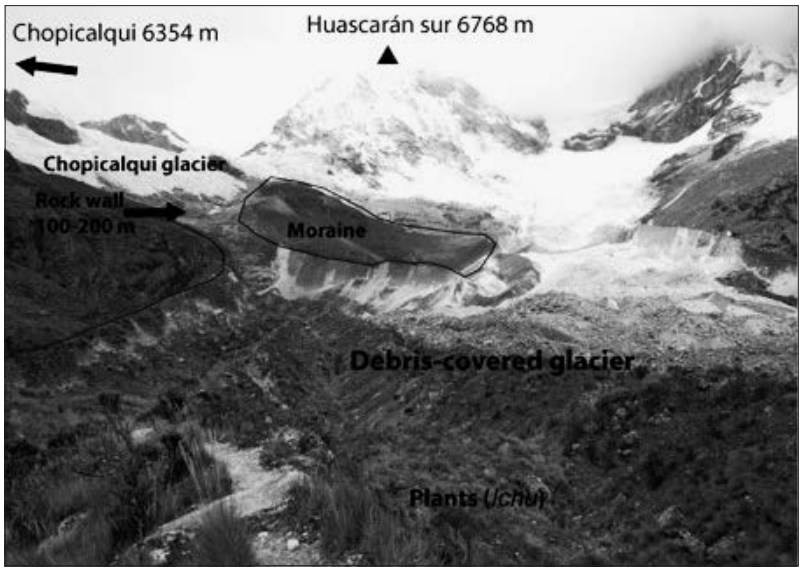

Fig. 11. Debris-covered glacier between Chopicalqui and Huascarán in 2013. Photo: W. Silverio.

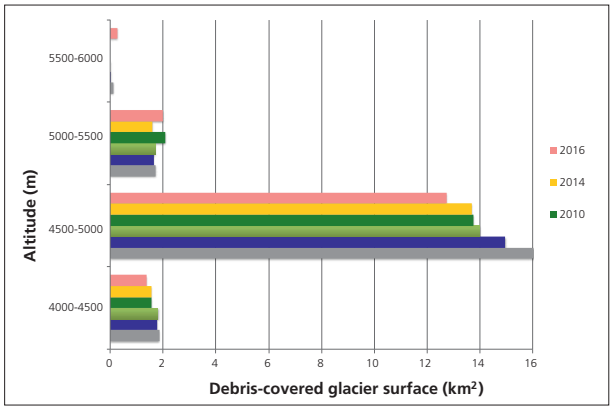

Fig. 12. Debris-covered glacier cover evolution by altitude between 1987 and 2016 (km²) in Cordillera Blanca.

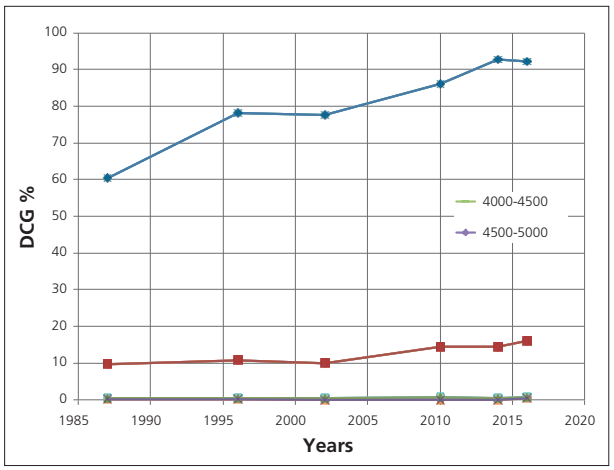

Fig. 13. Debris-covered glacier cover evolution (in % of total cover) by altitude between 1987 and 2016 in Cordillera Blanca.

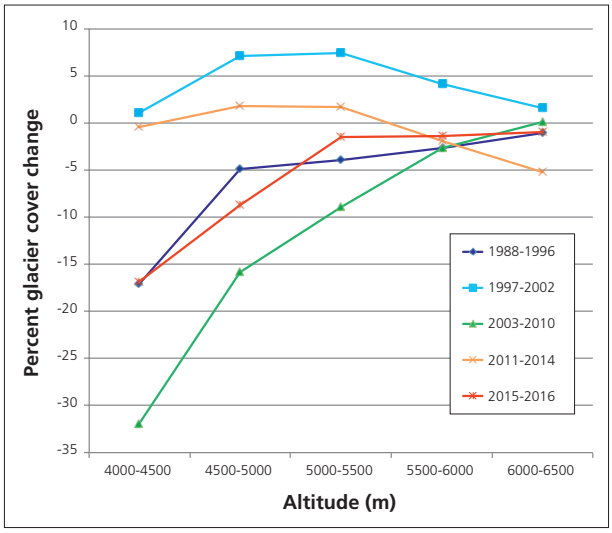

*Fig. 14. Evolution of glacier cover change (*PGCC*; in %) with altitude for five periods between 1988 and 2016*

of only 2 % between the *NDSI* and the B4/B5 results, which makes the resulting estimates quite comparable. Our own results for 1987, 1996 and 2002 confirm this. Allowing for rock outcrops within the glacier limits (which was not considered in a previous study (Silverio and Jaquet 2005)) decreased the glacial cover estimate in 1987 and 1996 by only 1.7 %.

Pooling together the various glacier cover estimates provides a historical record of the cryosphere in Cordillera Blanca between 1930 and 2016 (see Table 3). The decreasing trend in glacier cover is quite clear in Fig. 5. Whatever the method applied, all authors agree about the reality of glacial retreat during recent decades (Silverio and Jaquet 2005; UGRH 2010; 2013; Racoviteanu et al. 2008; Georges 2004; 2005). It is interesting, however, to examine the differences in various glacial cover estimates (Table 3 and Fig. 5). According to Georges (2004), the glaciers of the Cordillera Blanca covered an area of around 800-850 km² in 1930, which is the only data available for this period. For 1970, the estimates by Georges (2004) and Ames et al. (1988) differ by 51 km², which is insignificant due to the mapping methodologies (manual delineation on aerial photographs). In 1991, Georges (2004) carried out glacial mapping manually on a colored composite of SPOT images from July 22, 1991 (covering the northern part of the Cordillera Blanca,) and June 2, 1987 (covering the southern part), a difference of four years. These images do not cover the entire Cordillera Blanca, and the area of glaciers outside these images was extrapolated by multiplying the area from 1970 by a factor of 0.88 (rate of retreat = 1990 area divided by 1970 area) of Huascarán massif (Kaser et al. 1996). In addition, Georges (2004) believes that the cartographic error is less than 3 % (19 km²). Given that the area of ice cover for 1990 was based on a 20 m-pixel resolution, we believe that the cartographic error must be greater than 20 km². In spite of these approximations, Georges (2004) estimate of 620 km² falls within the uncertainty margin of our own computed value for 1987 (618 km² ± 60).

Between 1996 and 2003, all estimates are in the range of 528-600 km². The difference in glacial cover between Racoviteanu et al. (2008) (569 km² ± 21) and UGRH (2010) (528 km²) is probably due to the methods and the satellite images used. Racoviteanu et al. (2008) based their glacial mapping on SPOT images (20 m pixel) and had the same problem as Georges (2004): for the glaciers not covered by the images, they also resorted to an extrapolation. In contrast, UGRH (2010) used Aster images (15 m pixel). The present glacial cover estimate for 2016 (449 km² ± 56) is the lowest of the whole series.

In a recent study, Burns and Nolin (2014) show that Cordillera Blanca's glaciers covered 643.5 km^2 in 1987, 584 km^2 in 1996 and 482.4 km^2 in 2010. These differ from our own estimates by 2 % for 1987, 1 % for 1996, and 1 % for 2010. These small discrepancies are well within the error margins inherent to the methods used (atmospherically corrected images and NDSI by Burns and Nolin (2014), *vs*. a combination of NDSI and TM4/TM5 computed on raw DNs). Moreover, the dates are not the same for the 1987 images. For the estimation of Cordillera Blanca's glacial cover, UGRH (2010) considered only glacier bodies ≥ 0.005 km^2; Racoviteanu et al. (2008) and Burns and Nolin (2014) fixed the limit at ≥ 0.01 km^2 in contrast with the value of ≥ 0.0027 km^2 (3 pixel) in this work.

The reported uncertainties must be considered when looking at the differences between these estimates, whether across time within a given study or among various authors at a given date (Fig. 5). As indicated in table 3, this information is available in only the present study and from Racoviteanu et al. (2008) and is expressed by the Perkal or epsilon band in both instances. To quote Goodchild (1993), "Although the Perkal band is a useful concept in describing errors in the representation of complex objects and in adapting GIS processes to uncertain data, it falls short of a stochastic process model of error". As a consequence, the Perkal band will greatly overestimate the true uncertainty. This means that the 8-12 % uncertainties affecting our glacial cover estimates (table 3) should be substantially reduced, thereby giving better credit to the reality of the overall multi-annual decreasing trend in Fig. 5.

The second-degree fit represented on this figure (dotted line) indicates a nonlinear glacial shrinkage accelerating with time. The smoothed rate of change (expressed by the first derivative GC') changes from -1 km^2 y^{-1} in the 30s to -6 km^2 y^{-1} in this century. Other studies have reported similar acceleration (see Paul and Haeberli 2008).

The reality of glacial shrinkage is substantiated by ground observation by Peruvian glaciologists of the Broggi (Fig. 6) and Pastoruri glaciers (Figs. 7-9). The ground data are all within the uncertainty limits of satellite-derived estimates.

6.2. Evolution of glacier cover by altitude

Glacier cover has decreased at all altitudes between 1987 and 2016 (Fig. 10A), although to varying degrees. The change per altitude (Table 4a, last column) ranges from -53 % at 4500 m to -5 % at 6000 m, showing a clear dependence on altitude. Over time, the percentage of glacier cover steadily decreases between 4500-5000 m, which is compensated by an increase above 5000 m (Figure 10B). An interesting feature is visible on the graph of Figure 10A for altitudes between 4500 and 5000 m and even more between 5000 and 5500 m: there is a trend reversal in 2002 and 2014 with a small regrowth of glacial cover that matches a similar reversal in Figure 5. This phenomenon can be interpreted in relation to ENSO episodes.

Although the total glacier cover decreased by 27 % between 1987 and 2016 (Table 4B), the DCGs decreased by only 17 % (Table 5). This smaller ablation is also visible between 4000 m and 5500 m and is due to the protection by the rock debris cover from solar radiation. Pratap et al. (2015) observed 37 % less ablation of debris-covered ice than clean ice in the Himalayas. This effect was particularly strong in the lowest-altitude glacier tongues (Collier et al. 2015) in the absence of supraglacial lakes (Basnett et al. 2013), where it can lead to fragmentation of the snout. As a consequence, the proportion of DCG's at lower altitudes increases with time, as shown in Fig. 13, reaching 90 % between 4000 and 4500 m. The images from 2010 show a separation from the main Chopicalqui glacier for the debris-covered glacier located between Chopicalqui and Huascarán (Llanganuco valley; for the location see Fig. 1; for descriptions see Silverio and Jaquet 2003; 2009; Silverio 2003). During our 2013 field trip, we observed that both parts are now separated by a rock wall 100-200 m high (Fig. 11) and that the lowermost part is being colonized by vegetation (mostly *Ichu*). In 2003 UGHR (2010) identified 19 debris-covered glaciers (11 km^2). Other studies mention neither the number nor the surface area of these glaciers (Racoviteanu et al. 2008; Burns et Nolin 2014).

The glacial cover change for 1988-1996, 2003-2010, and 2015-2016 (Fig. 14) is inversely related to the altitude, but not linearly, and it is similar to the overall trend observed in the Swiss Alps between altitude and thickness losses (Paul and Haeberli 2008, fig. 2).

6.3. ENSO and Cordillera Blanca.

El Niño and La Niña correspond to warm and cold phases of ENSO, respectively. ENSO has an impact on the temperature and precipitation in the Andean tropical and sub-tropical regions (Vuille et al. 2008). These hydroclimatic perturbations control the glacier mass balance of Andean glaciers (Francou et al. 1997) through reinforcement of the subtropical air pressure, which weakens the displacement of humid air from the Amazon towards the Andes. In Cordillera Blanca, La Niña is associated with temper-

atures lower than normal. In contrast, El Niño episodes are systematically associated with an increase in air temperature, depending on the event's magnitude. At Queracocha station (4050 m) the mean temperature can rise by 0.2-0.6°C during El Niño (Silverio 2007), causing the glaciers' equilibrium line to rise between 150 and 300 m (Francou et al. 1997). In these conditions, rains can fall in the ablation zone and enhances the retreat.

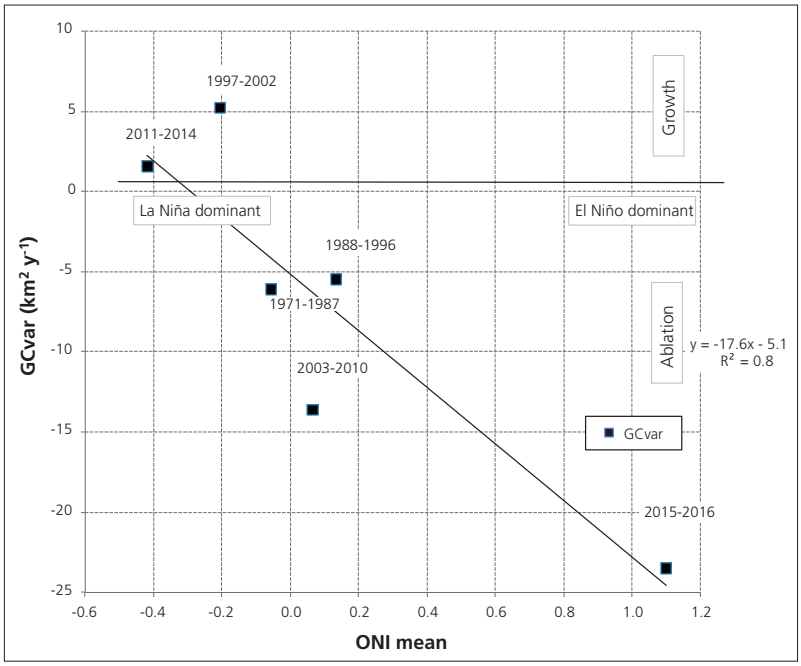

*Fig. 15. Relationship between the Oceanic Niño Index (*ONIm; *see definition in text) and* GCvar, *the yearly variation of glacial cover in Cordillera Blanca for six periods between 1971 and 2016. The correlation coefficient is significant at* p = *0.95.*

However, as far as rainfall is concerned, it is very difficult to characterize an El Niño event in the Cordillera Blanca. It seems that the massif is a transition zone between a wetter north and a drier south (Pouyaud et al. 2003). As shown in Fig. 4, precipitation varies during El Niño episodes (Silverio 2007). Glaciological observations of the Shallap glacier (4750m) by Maussion et al (2015) indicate a deficit in precipitation during El Niño years and an excess during La Niña. They have also demonstrated that the influence of ENSO is stronger at lower altitudes but remains detectable at higher elevations.

In Equator and Bolivia, ENSO has a similar impact on glaciers (negative mass balance during El Niño and positive or near-equilibrium during La Niña) (Francou et al. 2003; 2004). The same phenomenon has been observed in Cordillera Blanca (Vuille, et al. 2008; Kaser et al. 2003).

We have attempted to quantify the antagonistic influences of the El Niño and La Niña episodes by regressing *GCvar* against the mean of *ONIm* (Fig. 15). For the six periods studied, the clearly negative values of *ONIm* indicate a predominance of La Niña inducing a regrowth of glacier cover (1997-2002 and 2011-2014), whereas a strong shrinkage occurs (-23 km^2 y^{-1} in 2015-2016) due to dominant El Niño episodes. The linear relationship fitted to the relatively small number of *ONIm/GCvar* pairs makes sense (Francou et al. 2004) and may be provisionally accepted, but with due regard to the following: (a) How effectively *ONIm* represents the action of ENSO on glacier cover variation which might vary with the duration of the periods considered (from 22 to 204 months). The longer the duration, the more chances there are to have a mix of El Niño and La Niña acting in an antagonistic way (Table 6). (b) Over a given period, the order of occurrences of El Niño and La Niña could play a part in the magnitude of *GCvar*. (c) The explaining power of the relationship suggested in Fig. 5 is bound to be limited by the uncertainty inherent to *GCvar*, which is dependent on the uncertainty of GC represented by error bars based on the Perkal band in Fig. 5. This concept lacks a solid statistical justification, so we cannot propagate the error from GC to *GCvar* at this stage or precisely explain the spread of *ONIm/GCvar* pairs from either side of the trend line. (d) The variability of precipitations documented within the Cordillera Blanca (Fig. 4) could also blur the causal chain between *ONIm* and *GCvar*. Clearly, further exploration is needed for the validity and possible predictive power of the Oceanic Niño Index on the rate of glacier cover change.

The partition between negative and positive *ONIm* values (Fig. 15) can explain the two families of PGCC curves in Fig. 14. In 1997-2002 and 2011-2014, when *ONIm* < 0, La Niña induced a maximal glacier cover regrowth between 4500 and 5500 m. It also produced a transient trend reversal in the glacier cover evolution by altitude (Fig. 10A), while it reduced the number of ice bodies in 2002 and stabilized their number in 2014 through favoring the coalescence of glacier tongues (Fig. 5).

The trend reversals in glacier cover observed in recent years (Fig. 5) bear witness to their rapid reaction to changing climatic conditions such as ENSO (Kaser et al. 2003; Vuille et al. 2008). To quote Kaser et al. (2003), "After the 1997/98 El Niño, the

glaciers in the Cordillera Blanca have experienced a mass gain leading to tongue advances which have started in 2001 (G. Kaser, field observations in May 2001)". After El Niño (May 1997 - April 1998). May-June 1998 were considered as neutral phase (NOAA, 2016), and La Niña took place in the Andes for a long period (July 1998 - March 2001). Then, during La Niña 1998/2001, glaciers gained in their mass and surface, as recorded by the satellite images of 2002. This situation can explain the regrowth of glacier cover between1997 and 2002.

7. Conclusions

By virtue of their repeatability, satellite images provide a diachronic record of the general state of glaciers. As such, they represent an important source of information and provide the only possible overview of remote mountain ranges such as Cordillera Blanca. The satellite images Landsat TM, ETM+, and OLI with a 30-m pixel resolution allow cartographic monitoring of the glaciers with an uncertainty of ± 10 %, as expressed by the Perkal band. However, the true error is probably lower in reality. Despite their slightly lower resolution compared to that of Spot images (20 m) and Aster (15 m), the much larger size (180 x 180 km) of Landsat imagery allows for a larger and cheaper coverage.

The exclusion of rock outcrops inside the glacier border only decreased the previously reported glacial cover by 10 km^2 in 1987 and 1996. Overall, in spite of differences in mapping methodologies, our glacial cover estimates and those of other authors are comparable, given the mentioned uncertainty margin. In particular, glacier cover estimates obtained using the Landsat near-infrared band ratio and normalized difference snow index are not significantly different. The general decrease in glacial cover seen in satellite imagery is beyond doubt, and it is confirmed by surveys carried out in the field: The Cordillera Blanca glacierized area was around 825 km^2 in 1930, and only 449 km^2 in 2016, representing an overall loss of 46 % in 86 years. The trend appears to be nonlinear and was modeled by a second-degree polynomial indicating an increase in loss rate with time, reaching 23 $km^2\ y^{-1}$ between 2015 and 2016 *vs.* 5 $km^2\ y^{-1}$ in the 80's. The decrease in cover is notable between 4500-5000 m and 5000-5500 m, and the latter altitude class is becoming more dominant with time (over 60 %).

Upon superposing the overall decrease of glacier surface between 1987 and 2016 (negative changes), there are two trend reversals showing a positive change in cover between 1997-2002 and 2011-2016, as well as a lower number of ice bodies, which mostly occurs between 4500 and 5000 m. Quantification of the role of ENSO in short-frequency glacier cover variation has been attempted by regressing the rate of change with the Oceanic Niño Index. This relationship shows a certain amount of dispersion that has to be explained but is nonetheless significant.

Acknowledgments

We would like to express our gratitude to Bernard Pouyaud (IRD-Montpellier-France) for providing climate information, as well as to Abel Rodriguez, EGENOR former collaborator, for providing complementary climate information. We are grateful to Mark A. Ernste, former collaborator of UNEP/GRID-Sioux Falls (DEWA), USGS EROS Data Center, SD Dakota (USA) for providing the 1975 Landsat images. We also thank the United States Geological Survey (USGS) for the 1987, 1996, 2002, 2010, 2014, and 2016 Landsat images, which were obtained via their web site http://glovis.usgs.gov/. Field information provided by Nelson Santillán, former collaborator of UGRH-Huaraz (INRENA), is also gratefully acknowledged.

References

- **Albert T.** 2002. Evaluation of remote sensing techniques for ice-area classification applied to the tropical Quelccaya ice cap, Peru. *Polar Geography*, 26(3) : 210-226.
- **Ames A, Dolores S, Valverde A, Evangelista P, Corcino J, Ganvini W, Zuñiga J.** 1988. *Glacier inventory of Peru*. Empresa Regional Electronorte medio HIDRANDINA S. A., Unit of glaciology and Hydrology Huaraz, Peru, 105 p.
- **Basnett S, Kulkarni AV, Bolch T.** 2013. The influence of debris cover and glacial lakes on the recession of glaciers in Sikkim Himalaya, India. *J. of Glaciology*, 59(218) : 1035-1046.
- **Bonn F, Rochon G**. 1993. Précis de Télédétection, volume 1 : principes et méthodes. Presses de l'Université de Québec et AUPELF, Sainte-Foy, 485 pp.
- **Burns P, Nolin A.** 2014. Using atmospherically-corrected Landsat imagery to measure glacier area change in the Cordillera Blanca, Peru from 1987 to 2010. *Remote Sensing of Environment*, 140 : 165-178.
- **Bury J, Mark BG, Carey M, Young KR, McKenzie JM, Baraer M, French A, Molly HP.** 2013. New Geographies of Water and Climate Change in Peru : Coupled Natural and Social Transformations in the Santa River Watershed. *Annals of the Association of American Geographers*, 103 (2) : 363-374.
- **Cai W, Santoso A, Wang G, Yeh S-W, An S-I, Cobb K M, Collins M, Guilyardi E, Jin F-F, Kug J-S, Lengaigne M, McPhaden M J, Takahashi K, Timmermann A, Vecchi G, Watanabe M, Lixin W.** 2015. ENSO and greenhouse warming. *Nature climate change*, 5 : 849-859. DOI : 10.1038/NCLIMATE2743
- **Capotondi A, Guilyardi E, Kirtman B.** 2013. Challenges in understanding and modeling ENSO. PAGES news 21(2) : 58-59.
- **Colby JD.** 1991. Topographic Normalization in Rugged Terrain. *Photogrametric Engineering and Remote Sensing*, 57(5) : 531-537.
- **Collier E, Maussion F, Nicholson LI, Mölg T, Immerzeel WW, Bush ABG.** 2015. Impact of debris cover on glacier ablation and atmosphere-glacier feedbacks in the Karakoram. *The Cryosphere Discuss.*, 9 : 2259-2299.
- **Dymond JR, Shepherd JD.** 1999. Correction of the Topographic Effect in Remote Sensing. *IEEE Transactions on Geoscience and Remote Sensing*, 37(5) : 2618-2619.
- **Francou B, Ribstein P, Pouyaud, B.** 1997. La fonte des glaciers tropicaux. *La Recherche*, 302 : 34-37.
- **Francou B, Vuille M, Wagnon P, Mendoza J, Sicart JE**. 2003. Tropical climate change recorded by a glacier in the central Andes during the last decades of the 20th century : Chacaltaya, Bolivia, 16S. *J. Geophys. Res.* 108, D5, 4154. doi :10.1029/2002JD002959.
- **Francou B, Vuille M, Favier V, Cáceres B.** 2004. New evidence for an ENSO impact on low latitude glaciers : Antizana 15, Andes of Ecuador, 0°28'S. *J. Geophys. Res.* 109, D18106. doi : 10.1029/2003JD004484.
- **Francou B, Wagnon P.** 1998. *Cordillères andines, sur les hauts sommets de Bolivie, du Pérou et d'Equateur*. Glénat, Grenoble, 127 p.
- **Georges C.** 2004. The 20th century glacier fluctuations in the tropical Cordillera Blanca (Perú). *Arctic, Antarctic and Alpine Research*, 36(1) : 100-107.
- **Georges C.** 2005. *Recent glacier fluctuations in the tropical Cordillera Blanca and aspects of the climate forcing*. Ph.D. thesis, University of Innsbruck, Institute of Geography, Tropical Glaciology Group, Austria, 169 p.
- **Goodchild MF.** 1993. Data models and data quality : problems and prospects. In M.F. Goodchild, B.O. Parks, and L.T. Steyaert, editors, *Environmental Modeling with GIS*, Oxford University Press, New York pp 94–104
- **Hall DK, Ormsby JP, Bindschadler RA, Siddalingaiah H.** 1987. Characterization of snow and ice reflectance zones on glacier using Landsat Thematic Mapper Data. *Annals of Glaciology*, 9 : 104-108.
- **Hall DK, Riggs GA, Salomonson VV.** 1995. Development of methods for mapping global snow cover using Moderate Resolution Imaging Spectroradiometer (MODIS) data. *Remote Sensing of Environment*, 54 : 127-140.
- **Kaser G, Ames A, Zamora M.** 1990. Glacier fluctuations and climate in the Cordillera Blanca, Perú. *Annals of Glaciology*, 14 : 136-140.
- **Kaser G, Georges C, Ames A.** 1996. Modern glacier fluctuations in the Huascarán-Chopicalqui massif of the Cordillera Blanca, Perú. *Zeitschrift für Gletscherkunde und Glazialgeologie*, 32 : 91-99.
- **Kaser G, Juen I, Georges C, Gómez J, Tamayo W.** 2003. The impact of glaciers on the runoff and reconstruction of mass balance history from hydrological data in the tropical Cordillera Blanca, Perú. *Journal of Hydrology*, 282 : 130-144.
- **Kaser G, Osmaston H.** 2002. *Tropical Glaciers*. Cambridge : Cambridge University Press and UNESCO, Cambridge, 207 p.
- **Maussion F, Gurgiser W, Grobhauser M, Kaser G, Marzeion B.** 2015. ENSO influence on surface energy and mass balance at Shallap Glacier, Cordillera Blanca, Peru. *The Cryosphere*, 9 : 1663-1683. www.the-cryosphere.net/9/1663/2015 doi : 10.5194/tc-9-1663-2015
- **National Aeronautics and Space Administration (NASA).** 2016. Landsat Missions : Imaging the Earth Since 1972. Available online http ://landsat.usgs.gov//about_mission_history.php (Last accede on February 25, 2016)
- **National Oceanic and Atmospheric Administration (NOAA).** 2016. ENSO : Cold & Warm Episodes by Season. http ://www.cpc.noaa.gov/products/analysis_monitoring/ensostuff/ensoyears.shtml (Acceded on October 25, 2016)
- **Paul F.** 2000. Evaluation of different methods for glaciers mapping using Landsat TM. Proceeding of EARSeL-SIG-Workshop Land Ice and Snow, Dresden/FRG, June 16-17.
- **Paul F.** 2002. Combined Technologies Allow Rapid Analysis of Glacier Changes. *EOS, Transactions, American Geophysical Union*. 83(23) : 253 and 260-261.
- **Paul F.** 2003. *The new Swiss glacier inventory (2000). Application of Remote Sensing and GIS.* Ph.D. thesis, University of Zürich, Switzerland, 199 p.

- **Paul F, Haeberli W.** 2008. Spatial variability of glacier elevation changes in the Swiss Alps obtained for two digital elevation models. *Geoph. Res. Letters*, 35, L21502, 5 p.
- **Paul F, Kaab A, Maisch M, Kellenberger T, Haeberli W.** 2002. The new remote sensing-derived Swiss glacier inventory. I. Methods. *Annals of Glaciology*, 34 : 355-361.
- **Paul F, Kaab A, Maisch M, Kellenberger T. Haeberli W.** 2004. Rapid Disintegration of alpine glaciers observed with satellite data. *Geophy. Res. Lett.*, 31, L21402, doi :10.1029/2004GL020816.
- **Pouyaud B, Vignon F, Yerren J, Suarez W, Vega F, Zapata M, Gomez J, Tamayo W, Rodriguez, A.** 2003. Glaciares y recursos hídricos en la cuenca del río Santa. IRD-SENAMHI-INRENA report (internal document), 66 p.
- **Pratap B, Dobhal DP, Mehta M, Bhambri R.** 2015. Influence of debris cover and altitude on glacier surface melting : a case study on Dokriani Glacier, central Himalaya, India. *Annals of Glaciology*, 56(70) : 9-16.
- **Racoviteanu A, Arnaud Y, Williams MW, Ordoñez J.** 2008. Decadal changes in glaciar parameters in the Cordillera Blanca, derived from remote sensing. *Journal of Glaciology*, 54(186) : 499-510.
- **Rees WG.** 2006. Physical principles of remote sensing. Cambridge University Press, 3rd edition. Cambridge, 460 p.
- **Sandmeier S.** 1995. *A Physically-Based Radiometric Correction Model, Correction of Atmospheric and Illumination Effects in Optical Satellite Data of Rugged Terrain*. Remote Sensing Series, vol. 26, Remote Sensing Laboratories, Department of Geography, University of Zurich, 42 p.
- **Schauwecker S, Rohrer M, Acuña D, Cochachin A, Dávila L, Frey H, Giráldez C, Gómez J, Huggel C, Jacques-Coper M, Loarte E, Salzmann N, Vuille M.** 2014. Climate trends and glacier retreat in the Cordillera Blanca, Peru, revisited. *Global and Planetary Change* 119 : 85-97.
- **Silverio W.** 2003. *Atlas del Parque Nacional Huascarán – Cordillera Blanca – Perú*. Silverio, W. (Ed.), Lima, 72 p.
- **Silverio W.** 2007. "*A GIS for the sustainable management of the water resources in Cordillera Blanca (Peru)*" (in French). Ph.D. thesis in Geography, University of Geneva, Switzerland, 234 p.
- **Silverio W, Jaquet J-M.** 2003. Cartographie provisoire de la couverture du sol du Parc national Huascarán (Pérou), à l'aide des images TM de Landasat. *Télédétection*, 3(1) : 69-83.
- **Silverio W, Jaquet J-M.** 2005. Glacial Cover Mapping (1987 – 1996) of the Cordillera Blanca (Peru) Using Satellite Imagery. *Remote Sensing of Environment*, 95 : 342-350.
- **Silverio W, Jaquet J-M.** 2009. Prototype land-cover mapping of the Huascarán Biosphere Reserve (Peru) using a digital elevation model, and the NDSI and NDVI indices. *Journal of Applied Remote Sensing*, 3, 0335516 (2009), DOI :10.1117/1.3106599.
- **UGRH (Unidad de Glaciología y Recursos Hídricos, Autoridad Nacional del Agua).** 2010. *Inventario de glaciares Cordillera Blanca*. Unidad de Glaciología y Recursos Hídricos, Huaraz, 74 p, (unpublished).
- **UGRH (Unidad de Glaciología y Recursos Hídricos, Autoridad Nacional del Agua).** 2013. *Inventario Nacional de glaciares y lagunas : Glaciares*. Autoridad Nacional del Agua, Huaraz-Lima, (unpublished).
- **Vaughan DG, Comiso JC, Allison I, Kaser G, Kwok R, Mote P, Paul F, Ren J, Rignot E, Solomina O, Steffen K, Zhang T.** 2013. Observations : Cryosphere. In Stocker, T.F., D. Qin, G.-K Plattner, M. Tignor, S.K. Allen, J. Boschung, A. Nauels, Y. Xia, V. Bex and P :M. Midgley (eds), Climate Change 2013 : the Physical Science Basis. Contribution of Working Group I to the Fifth Assessment Report of the Intergovernmental Panel on Climate Change. Cambridge University Press, Cambridge, New York, pp 317-382.
- **Vuille M, Kaser G, Juen I.** 2008. Glacier mass balance variability in the Cordillera Blanca, Peru and its relationship with climate and the large-scale circulation. *Global Planetary Change*, 62 : 14-18.
- **Wagnon P.** 2001. El Niño et La Niña : les enfants terribles. *Verticalroc*, sept./oct, 38-39.
- **Williams RS, Hall DK, Benson CS.** 1991. Analysis of glacier facies using satellite techniques. *Journal of Glaciology*, 37(125) : 120-128.